

Double-Side Feeding and Reactive Power Compensation Using the Railway Interline Power Flow Controller

António Pina Martins ^{1,2,*}  and Vítor Alves Morais ³ 

¹ Faculty of Engineering, University of Porto, Rua Dr. Roberto Frias, s/n, 4200-465 Porto, Portugal

² SYSTEC—Research Center for Systems and Technologies, 4200-465 Porto, Portugal

³ NomadTech, Rua do Ferroviário, Gatões, 4460-020 Guifões, Portugal; vitor.morais@nomadtech.pt

* Correspondence: ajm@fe.up.pt

Abstract: This paper gives an overview of the operating characteristics of the railway interline power flow controller (RIPFC) regarding the capability of transferring active power between two sections of an electrified railway line separated by a neutral zone and proposes its use for compensating the power factor at the substation instead of regulating the voltage level at the neutral zone. The basic analysis is based on simplified steady-state models for the energy supply architecture, while detailed time-domain simulations are used for more realistic tests. The paper mainly focus on active power balancing between two neighbouring substations and the global losses in the system. Other functionalities of the RIPFC system are also analysed, like reactive power compensation at the substations. The paper presents the main operating principles of the system, shows results for some representative scenarios (generic and reduced) and discusses the results. The most relevant conclusions are related to substation active power balancing and peak shaving, power factor compensation in the substation, voltage stability at the neutral zone and system power losses.

Keywords: double-side feeding; losses; neutral zone; power factor; railway electrification; voltage stabilization



Citation: Martins, A.P.; Morais, V.A. Double-Side Feeding and Reactive Power Compensation Using the Railway Interline Power Flow Controller. *Eng* **2024**, *5*, 70–90. <https://doi.org/10.3390/eng5010005>

Academic Editor: Antonio Gil Bravo

Received: 13 November 2023

Revised: 15 December 2023

Accepted: 22 December 2023

Published: 27 December 2023



Copyright: © 2023 by the authors. Licensee MDPI, Basel, Switzerland. This article is an open access article distributed under the terms and conditions of the Creative Commons Attribution (CC BY) license (<https://creativecommons.org/licenses/by/4.0/>).

1. Introduction

Modern electrified railway networks systems are complex distributed power systems facing different challenges today and in the near future. These challenges appear in several domains, like the need to incorporate and deal with distributed renewable energy sources [1] and to increase the flexibility and resilience of the energy supply [2] during higher power consumption. At the same time, the growing number of passengers pushes towards increasing the trains' speed and traffic density but keeping the reliability, availability and safety of the energy supply at the highest levels, namely when crossing neutral zones [3].

In electrified railway networks, the active power supplied by one substation (SST) mainly depends on the number of trains present in the line and the power consumption of each one. Thus, there are situations in which an SST is supplying high power and eventually is in an overload condition. On the contrary, in another situation, the SST can be supplying very low power. An additional issue can be considered: situations when a train is in braking/regenerative mode and some amount of active power is injected into the catenary [4,5]. As known, overload conditions are not particularly appreciated and should be avoided as much as possible; they give origin to high losses, temperature rises and larger voltage drops, and the power peaks are penalized by the energy supplier [6,7].

Large asymmetries in the power supplied by two neighbouring SSTs contribute to a higher unbalance factor seen by the electric grid at either high-voltage (HV) or extra-high-voltage (EHV) levels [8]. Then, the Transmission System Operator or Distribution System Operator (TSO/DSO) could penalize the infrastructure manager according to the level

of the voltage unbalance factor [9]. Additionally, there are conditions when regenerative power is not allowed to be injected into the catenary system or, if allowed, is penalized. Then, the possibility of redirecting this energy should be considered [10–12]. Therefore, a power-electronics-based converter system connecting the two sections could manage both active and reactive power at the neutral zone [13–15].

This converter has been designated by several names: sectioning-post rail power conditioner (sp-RPC) [11], power transfer device (PTD) [15,16], and railway interline power flow controller (RIPFC) [17], which is the designation adopted in this work. The RIPFC system can play an important role in those scenarios, and some of them will be addressed in the following. The main objective of the RIPFC system is twofold: to be able to allow double-side feeding between two conventional (transformer-based) traction substations in a first step, thus supplying active power to the trains from two adjacent substations [15,18]; the second objective is to manage the reactive power in both nodes to which it is connected, thus stabilizing the voltage in those nodes [19].

The first objective can be fulfilled by the following actions that the system controller should allow: enable active power transfer between two collateral substations while respecting the following constraint: the overall losses should not be increased compared to those occurring in conventional feeding under the same traffic. Regarding the second objective (reactive power compensation in the two sectors to which it is connected) the main requirements are: the power factor at the substations should not be degraded compared to what it would have been in the conventional case under the same traffic. Additionally, the RIPFC system should: (i) be sized large enough to enable both of the above actions and (ii) improve the voltage level on both sectors (when loaded) compared to what would happen in conventional feeding. The fulfilment of these objectives is done with regard to other important requirements: the voltage magnitude, harmonic content and other disturbance levels should be met at all times [20,21]. The control strategy should be adapted to allow double-side feeding whenever it is useful and whenever it can bring benefits compared to the conventional situation.

The paper is organized as follows: in Section 2, the RIPFC system is described in both the power structure and the control modes and approaches; in Section 3, the voltage profile at the section end and the power factor at the substation are deduced using simplified diagrams. Section 4 presents a time-domain analysis using different compensation modes and traffic scenarios, and finally, in Section 5, the conclusions are drawn and discussed.

2. The RIPFC System

Architectures for supplying electrified railways vary to some extent. Indeed, the neutral zone can be a complex subsystem where the redirection of active power needs careful analysis due to the use of power electronic converters connecting different lines and sections [15]. In this section, we use a simplified architecture for demonstration purposes using steady-state phasor analysis. A basic insight regarding the possible advantages of using an RIPFC system can be made by analysing the circuit represented in Figure 1.

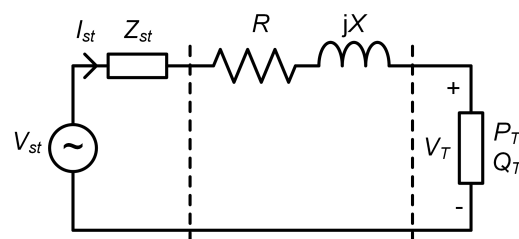


Figure 1. Substation with equivalent impedance, catenary lumped impedance and simplified train/load models.

The substation voltage, noted as V_{st} , provides current I_{st} to the load/train through the line/catenary with lumped impedance $Z = R + jX$. Impedance Z_{st} is fixed, and $R + jX$

represents the lumped impedance of the catenary at some distance from the substation where the train is located. Due to the line impedance, an absolute voltage drop occurs. The phasor diagram of the simplified circuit is shown in Figure 2, wherein Z_{st} has been neglected.

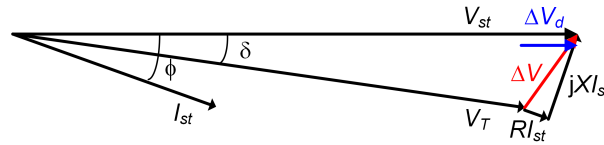


Figure 2. Simplified phasor diagram of substation and train voltages, line voltage drop and substation power factor.

The relative voltage drop ΔV is created and defined in (1). The calculation of the voltage drop is obtained using the phasor diagram as:

$$\Delta V = \frac{V_{st} - V_T}{V_{st}} = \frac{ZI_{st}}{V_{st}} \approx \frac{(R + jX)I_{st}}{V_{st}} \tag{1}$$

In the load, the relation between current and power is:

$$I_{st} = \left(\frac{S_T}{V_T} \right)^* = \frac{S_T^*}{V_T^*} = \frac{P_T - jQ_T}{V_T^*} \tag{2}$$

where * is the conjugate operator. Then, (1) can be rewritten as in (3):

$$\Delta V = \frac{P_T R + Q_T X}{V_{st} V_T^*} + j \frac{P_T X - Q_T R}{V_{st} V_T^*} \tag{3}$$

Equation (3) shows that the voltage drop has two components: a longitudinal one in-phase with V_{st} and a quadrature one. The last one is not of high relevance to system operation; it means that the instantaneous voltage has a phase lag in relation with the substation voltage. However, the in-phase voltage drop can substantially reduce the magnitude of the voltage at the pantograph. Assuming that the angle between V_{st} and V_T^* is small and that the magnitudes are similar, then (3) can be simplified as (4):

$$\Delta V \approx \frac{P_T R + Q_T X}{|V_{st}|^2} + j \frac{P_T X - Q_T R}{|V_{st}|^2} \tag{4}$$

The expansion of (3) would contain additional terms (coming from the product $V_{st} V_T^*$) that are not present in the approximated (4). However, these terms have a small contribution to the voltage drop. The assumption is used just to highlight the most relevant dependences between voltage drop and reactive power consumption through the term $Q_T X$. Focusing only on the in-phase voltage drop, it is given by (5) as:

$$\Delta V_d = \frac{P_T R + Q_T X}{|V_{st}|^2} \tag{5}$$

The voltage drop depends on the train's active and reactive power (P_T and Q_T , respectively), the catenary impedance $R + jX$ and the substation voltage V_{st} . With a moving train, the considered line impedance $R + jX$ changes according to the different train positions, thus affecting the drop. The farther the train is from the substation, the higher the voltage drop is. Therefore, the voltage drop ΔV_d is basically influenced by the train's active and reactive power and the train's position, assuming the substation voltage is almost constant.

In abstract, the RIPFC system can manage active and reactive power (P_C and Q_C , respectively). Then, if the converter could be connected in parallel with the load, the in-phase voltage drop would be given by (6):

$$\Delta V_d = \frac{(P_T + P_C)R + (Q_T + Q_C)X}{|V_{st}|^2} \tag{6}$$

The term P_C is an active power one; the RIPFC can, in fact, in some circumstances, control active power. However, the influence of this term is small since its contribution depends on R , which should be small. As an example, for a train with $PF = 0.9i$ and a typical catenary with $R = 0.15 \Omega / km$ and $X/R = 5.6$, the ratio between the two terms is $P_T R / Q_T X = 0.37$. This compensation type is discussed later and is used mainly for balancing the active power in the substations. The term Q_C is a compensating reactive power that can impose a null in-phase voltage drop. This means that the reduction in ΔV_d can be done by reactive power compensation, which can be achieved by the RIPFC system. Then, controlling the reactive power in (6) means controlling the voltage drop, although the total active power flow also has a role. The circuit diagram in Figure 3 includes a compensation current, I_c , in quadrature with voltage V_T (this is similar to the operation of the RIPFC converter but with regard to reactive power control only).

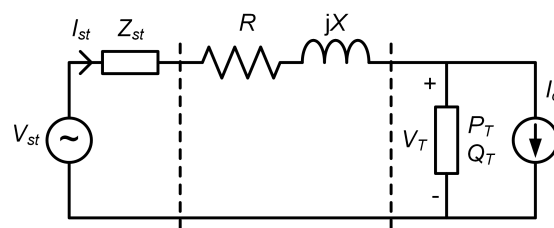


Figure 3. Simplified circuit diagram with compensation current.

If the goal is to impose a unitary power factor in the substation, then the resulting phasor diagram is represented in Figure 4.

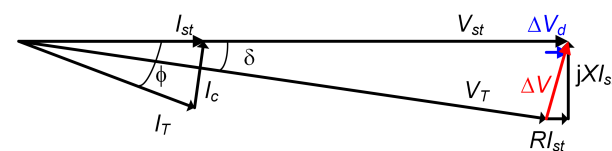


Figure 4. Simplified phasor diagram with compensation current.

It can be seen that the in-phase voltage drop is much smaller than before; the voltage at the connection point is higher. The RIPFC operates as an SVC but has the objective of imposing a unitary power factor at the substation; the voltage drop reduction is a positive side effect.

2.1. Structure and Capabilities

The basic power diagram of the RIPFC system is illustrated in Figure 5. Mainly, the RIPFC is constituted by two single-phase AC/DC/AC back-to-back converters with a common DC bus and two transformers to connect each converter to the catenary system. The specific converter structure can be based on different approaches, but the most common is a multilevel one built with cascaded H-bridges, multi-point clamped or modular multilevel converters. The transformers are designed according to the power level to be transferred between sections, the reactive power injected in the neutral zone and the voltage and current levels in the converters. Also, a parameter of high relevance in the RIPFC design both in the transformer and in the converters is the efficiency level in order to keep losses at a minimum and thus not compromise the overall losses when using the RIPFC system, particularly in the active power transfer mode.

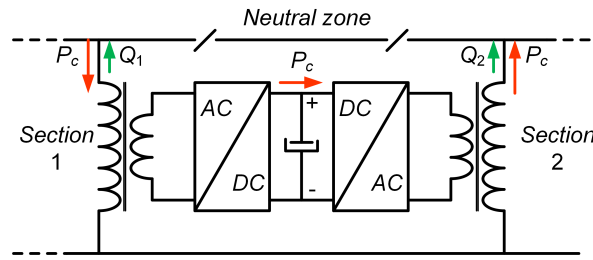


Figure 5. Main diagram of the power structure of the RIPFC system.

The RIPFC has two fundamental properties: it can inject variable reactive power into the end points of both sections where it is connected and independently for each section (Q_1 and Q_2), thus controlling the AC voltage level. It is very similar to the operation of a static var compensator (SVC) but using a PWM-controlled voltage-source converter. Additionally, if the DC buses of both DC/AC converters are electrically connected, then there is the possibility of transferring active power (P_c) between both AC sides and then reducing the power supplied by the heavily loaded SST and increasing the power of the lightly loaded one.

2.2. Voltage and Power Factor Characteristics

We first study the voltage and power factor characteristics of the system without any compensation. Then, a compensation strategy, as already pointed out before, is implemented and analysed. The base diagram is illustrated in Figure 6. In this work, we use the following assumptions: (i) the converter/compensator is located at the end of the section (the neutral zone (NZ)), (ii) the use of lumped parameters is valid (analysis at 50 Hz only), and (iii) only one load (train) is considered. The simplified analysis for operation without compensation is made using the diagram in Figure 6. For operation with reactive power compensation, the simplified diagram is shown in Figure 7. In the model, V_{st} is the open-circuit voltage of the substation, $Z_{st} = R_{st} + jX_{st}$ is the equivalent impedance of the circuit constituted by the TSO/DSO grid, Z_T is the equivalent impedance of the substation transformer, and $Z_{cat} = R_{cat} + jX_{cat}$ is the concentrated parameters of the catenary line, which depend on the distance between the load (train) and the substation. All these impedances are modelled by the impedance $Z_1 = R_1 + jX_1$. The load/train is modelled as an apparent load: $S_T = P_T + jQ_T$. Also, in this model, the distributed line capacitance is ignored. For the voltages, the following equation applies:

$$\underline{V}_{st} = (R_1 + jX_1)\underline{I}_{st} + \underline{V}_T \tag{7}$$

Load power is given by (8):

$$S_T = \underline{V}_T \underline{I}_T^* = P_T + jQ_T \tag{8}$$

Multiplying by \underline{I}_{st}^* in the voltage equation gives:

$$\underline{V}_{st} \underline{I}_{st}^* = (R_1 + jX_1)|\underline{I}_{st}|^2 + P_T + jQ_T \tag{9}$$

It should be mentioned that (9) can be solved for \underline{I}_{st} . In the subsequent analysis and results, we use the following assumptions: (i) V_{st} is constant, which is a simplification; and (ii) the apparent load power is an independent variable.

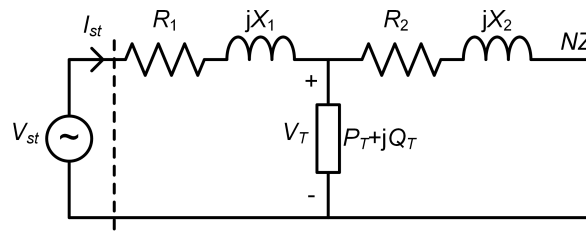


Figure 6. Simplified line diagram between the substation and the (disconnected) converter.

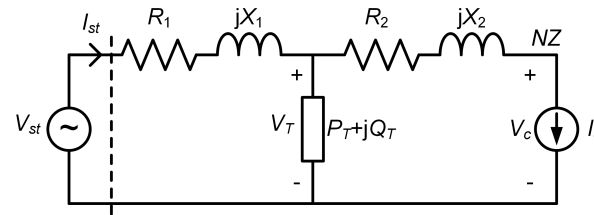


Figure 7. Circuit diagram in compensation mode (reactive power only).

2.2.1. Without Compensation

The first set of results addresses operation without compensation. The main parameters used for the substation are: $V_{st} = 27.5$ kV and $S_{st} = 16$ MVA. The catenary parameters are: $R_c = 0.15 \Omega / \text{km}$ and $X/R = 3$. For these results, the train is located 20 km away from the substation and has a nominal power of 8 MVA; its additional parameters are: fixed power factor $PF_T = 0.95i$.

Using (7) and (8), the evolution of the voltage magnitude at the connection point is expected to show an important drop almost linearly dependent on the train’s active power: in fact, it drops from 27.5 kV to 25.8 kV (Figure 8 (left), trace “uncompensated”). Additionally, we expect a reduction in the power factor at the substation level (it varies from 0.95i to 0.92i when P_T varies between 0 and 8 MW); this is also of concern since it implies higher currents and more losses in the system.

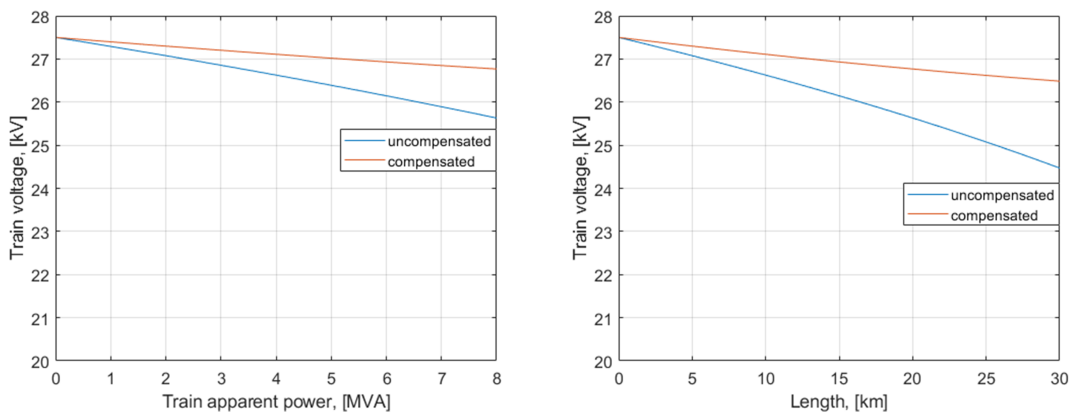


Figure 8. Train voltage when compensating the reactive power at the substation: (left) variable train power and fixed position (20 km) and (right) variable position and fixed power (8 MVA).

The second analysis, still without compensation, is related to the influence of the train’s position with the same parameters for the train voltage and substation power factor. For this illustration, the train consumes its nominal power ($S = 8$ MVA with $PF_T = 0.95i$) and travels along the whole catenary length. With constant apparent power, we expect both a reduction in the voltage at the pantograph connection and a reduction in the power factor at the substation. Specifically, when analysing the same parameters, the train voltage has a strong reduction when it travels near the neutral zone: it drops from 27.5 kV to 24.5 kV when the train moves from $d = 0$ to $d = 30$ km; after 20 km, the voltage reduction is quite

fast (Figure 8 (right), trace “uncompensated”). Regarding the substation power factor, the conclusion is similar; there is a more-pronounced reduction for larger distances: from 0.95i to 0.90i.

2.2.2. With Compensation

As known, and this is the main objective of an SVC, the RIPFC can be controlled in order to stabilize the voltage at the PCC (the neutral zone). Differently, the compensation strategy defined for demonstrating the RIPFC’s capabilities is to impose a unity power factor in the substation. The same two analyses are performed: variable train power with constant power factor ($PF_T = 0.95i$) maintaining the train in a fixed position and constant train power with variable position. In both cases, the other fundamental parameters were maintained. Figure 7 shows the associated diagram for the analysis.

The lumped impedance $R_2 + jX_2$ is the equivalent catenary impedance between the train position and the neutral zone. When using reactive power compensation, the active and reactive power balance equation is given by:

$$\underline{V}_{st}I_{st}^* = (R_1 + jX_1)|I_{st}|^2 + \underline{V}_T I_{st}^* \quad (10)$$

In the right loop, the power balance is given by:

$$\underline{V}_T I_c^* = (R_2 + jX_2)|I_c|^2 + \underline{V}_c I_c^* \quad (11)$$

The goal is to impose a unitary power factor at the substation using only reactive power, i.e.,

$$\Re\{\underline{V}_c I_c^*\} = 0 \quad (12)$$

Then, the three equations can be solved for I_{st} , \underline{V}_T and \underline{I}_c .

The results in Figure 8 (left) are to be compared (“uncompensated” versus “compensated” traces). As highlighted earlier, there is a much more constant voltage at the connection point, though this is somewhat dependent on the train’s power; the power factor in the substation is unitary as this was set as the objective of the compensation. For the other test, the train power is constant ($S = 8$ MVA, $PF_T = 0.95i$) and the position is variable. The results for the same variables are shown in Figure 8 (right).

The voltage profile provides the same conclusion: the voltage drop is quite small (less than 4%) in the whole section.

2.2.3. Discussion

Without compensation, the voltage drop at the load/train can be relevant and can impose limited power consumption in some conditions. Also, a reduction in the substation power factor is noticed, thus increasing the system losses. Both parameters depend on the train’s load factor, the catenary impedance and the train’s distance to the substation. The RIPFC converter, when compensating the power factor in the SST, not only can reduce the system losses through reduction in the current’s rms value but also highly limits the voltage drop at the pantograph connection.

The RIPFC’s operation is based on knowledge of the power factor in the substation. This variable must be supplied to the converter, which is tens of kilometres away from the substation; this implies that a fast and reliable communication link between the two is necessary [22]. This issue is out of the scope of this paper but will appear again when the RIPFC system is implemented to control the active power flow between the two sections.

3. Time-Domain Analysis

In this section we demonstrate, using time-domain simulations, the referred capabilities of the RIPFC system regarding active and reactive power management: balancing the active power supplied by both substations and imposing a near unitary power factor in the substation. Of course, the reactive power capability could be used to stabilize the voltage

at the neutral zone point, but this functionality is usually achieved by an SVC only [23,24]. As already pointed out in the phasor analysis, we will show that compensating the reactive power in the substation has a side effect of also stabilizing the voltage along the catenary.

3.1. Subsystem Models

The different subsystems used for time-domain simulations are: 1—TSO/DSO grid with an equivalent series impedance with a three-phase transmission line between the two substations; 2—single-phase transformer in each substation to feed the respective section and catenary system (1×25 kV) with distributed RLC parameters; 3—trains modelled as constant power loads that are active and reactive; 4—RIPFC system including transformers, DC/AC converters and a common DC bus.

The models are briefly described in the following.

3.1.1. TSO/DSO Grid with Equivalent Series Impedance

The model is a standard one and, for demonstration, the parameters given in Table 1 are used. The three-phase short-circuit power is $S_{sc} = 1800$ MVA with $X = 2.2 \Omega$ and X/R ratio = 5.6. In order to create a voltage drop between the input voltages of each substation, a loaded transmission line is introduced between the substations. When the line supplies its nominal power, a voltage drop of approximately 0.5% is created between the two substations.

Table 1. TSO/DSO line and SST transformer parameters.

| Parameter | TSO/DSO | SST Transf. |
|------------|--------------------|------------------------------|
| S_N | 250 MVA | 20 MVA |
| V_p/V_S | 63 kV | 63/27.5 kV |
| $R_p; R_S$ | 5.7 m Ω /km | 0.3 Ω ; 57 m Ω |
| $L_p; L_S$ | 0.1 mH/km | 25 mH; 5 mH |
| R_m | | 100 k Ω |

3.1.2. Substation Transformer and Catenary (1×25 kV) with Distributed RL Parameters

The substation transformers are equal, and its model has the parameters given in Table 1. As is common in conventional railway electrification, the primary winding of each transformer is connected to different phase pairs (e.g., RS and ST), i.e., a so-called single-phase connection scheme. The length of each section is considered to be the same and equal to 35 km. The whole section is divided into segments of 5 km each. The model of each segment is constituted by a line with distributed parameters (π -type) as given also in Table 1; the capacitance is neglected. A concentrated visualisation of the TSO/DSO line and the SST transformer parameters is given in Table 1.

3.1.3. Trains Modelled as Constant-Power Loads

A total of eight trains were considered: four in each section. All trains are modelled as constant-power loads with variable active power (in traction and regenerative braking modes) and a variable power factor according to standard EN 50388 [25]. The trains are located in different positions along the section, as detailed in the following subsections.

3.1.4. RIPFC System: Including Transformers, DC/AC Converters and a Common DC Bus

The transformer for connecting the RIPFC system to the two section ends (see Figure 5) has the parameters given in Table 2, where the magnetization inductance is neglected. For a global visualisation, the catenary and RIPFC parameters are shown in Table 2.

The structure of the DC/AC converters is not of high relevance for this work. As mentioned earlier, the structure of this converter can vary to a great extent: the most common is a multilevel one built with cascaded H-bridges, multi-point clamped or modular multilevel converters. Its structure has several factors influencing it: the number and sizing of semiconductors and capacitors, the DC bus voltage level, the switching frequency, the AC

filter sizing, the control method, etc. For simplification purposes, we choose the simplest one: the H-bridge. Thus, the additional parameters influenced by it and used in the work are given in Table 2.

Table 2. Catenary and RIPFC parameters.

| Parameter | Catenary | RIPFC |
|------------|------------------|--------------------------------|
| S_N | 20 MVA | 10 MVA |
| V_p/V_S | | 27.5/2.5 kV |
| $R_p; R_S$ | 0.1 Ω /km | 0.19 Ω ; 9.6 m Ω |
| $L_p; L_S$ | 0.8 mH/km | 1.6 mH; 0.08 mH |
| R_m | | 100 k Ω |
| V_{dc} | | 4500 V; 40 mF |
| F_s | | 2000 Hz |
| AC filter | | 1.5 mH; 5 m Ω |

3.2. Control Approach

The control approach for the RIPFC system is based on two control layers: converter control and active and reactive power control. Two different operating modes are possible: (i) reactive power flow control only and (ii) active and reactive power flow control. The two control modes can be schematically deduced from Figure 9 and are briefly described in the next subsections.

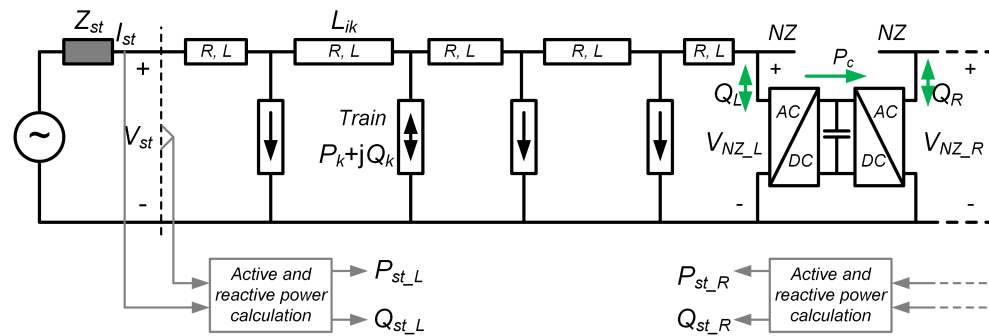


Figure 9. Simplified diagram of the connection between the RIPFC system and the left substation.

3.2.1. Reactive Power Control Only

In the first mode, the DC bus of each converter is separated from the other; the two converters operate independently; see Figure 9. The converter control is based on a single-phase equivalent-vector control approach for each converter [26]. The references for the left and the right converters are the DC bus voltage level (V_{dc}) and the reactive power level (Q_L and Q_R). According to [26], it is possible to have good dynamic performance for the control of these two variables using PI controllers. The reactive power the converter produces has a direct relation with the reactive power in the substation and, for control purposes, it is scaled to the injected current. In this mode, the constraint the RIPFC must satisfy is the maximum allowed current; in case the neutral zone voltage rises beyond limits, the RIPFC must be disconnected. As referred, the objective of reactive power injection into the section end is to obtain a unitary power factor at both substations, i.e., $Q_{st_L} = Q_{st_R} = 0$.

3.2.2. Double-Side Feeding and Reactive Power Control

In the second mode, the DC bus is common to both converters. Similarly, the converter control is based on a vector control approach.

The references for the left converter are the DC bus voltage level (V_{dc}) and the reactive power flow (Q_L); for the right converter, the references are the active power flow (P_C) and reactive power flow (Q_R). For the reactive power flow, the objective is the same as in the first mode (i.e., $Q_{st_L} = Q_{st_R} = 0$). Active power transfer has the objective of active

power control in the two substations, i.e., if both substations are balanced, then the power transferred in steady-state from the left section to the right one is given by (13):

$$P_c = \frac{P_{st_R} - P_{st_L}}{2} \tag{13}$$

where P_{st_R} is the total active power supplied by the right substation without balancing control and P_{st_L} is the total active power supplied by the left substation in the same condition. If losses are neglected, then the same expression can be approximated by:

$$P_c \approx \frac{\sum_{i=1}^{N_L} P_{TrL}(i) - \sum_{j=1}^{N_R} P_{TrR}(j)}{2} \tag{14}$$

where N_L is the number of trains in the left section, N_R is the number of trains in the right section, and $P_{Tr}(k)$ is the active power consumed/regenerated by train k . Then, P_c is the reference value for the right converter and is controlled in closed-loop.

It should be mentioned that a different objective than balancing the active power can be used; this only requires a higher-level command to implement it.

3.3. Results

In order to extensively study the different operating conditions that occur in a railway line, eight trains are used: four on each side of the neutral zone. The eight trains considered in the analysis start running at the times specified in Figure 10. Also, they are located in the positions shown in the same figure.

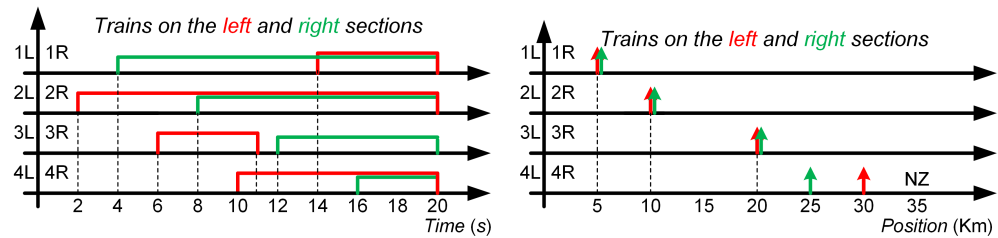


Figure 10. Start/stop times of trains (left) and their positions in their respective sections (right).

The power consumed/regenerated by each train and the associated power factors are presented in Table 3.

Table 3. Active and reactive power consumed by each train (L: left; R: right).

| Train | P, (MW) | Q, (MVA _r) | PF |
|-------|---------|------------------------|-------|
| Tr_1L | 2.0 | 1.0 | 0.9i |
| Tr_2L | 2.0 | 1.0 | 0.9i |
| Tr_3L | −4.0 | 0.0 | 1.0 |
| Tr_4L | 3.0 | 1.0 | 0.95i |
| Tr_1R | 1.0 | 0.75 | 0.8i |
| Tr_2R | 1.0 | 0.75 | 0.8i |
| Tr_3R | 4.0 | 1.3 | 0.95i |
| Tr_4R | −2.0 | 0.0 | 1.0 |

As mentioned, trains will have different active and reactive powers with different power factors, and some will be in braking mode. In the next paragraph, we show the results for three scenarios: without any compensation in order to establish the base results for comparison; when only compensating the reactive power in the substations; and when using full compensation, i.e., zero reactive power and active power balancing in each substation.

3.3.1. Without Compensation

The base scenario is without compensation. Using the parameters given before and the schedule and position also referred to earlier, the results are given in the following figures: Figure 11 shows the total active and reactive power in both substations; Figure 12 shows the power factor in the two substations; and Figure 13 shows the voltage in each substation and also in both sides of the the neutral zone.

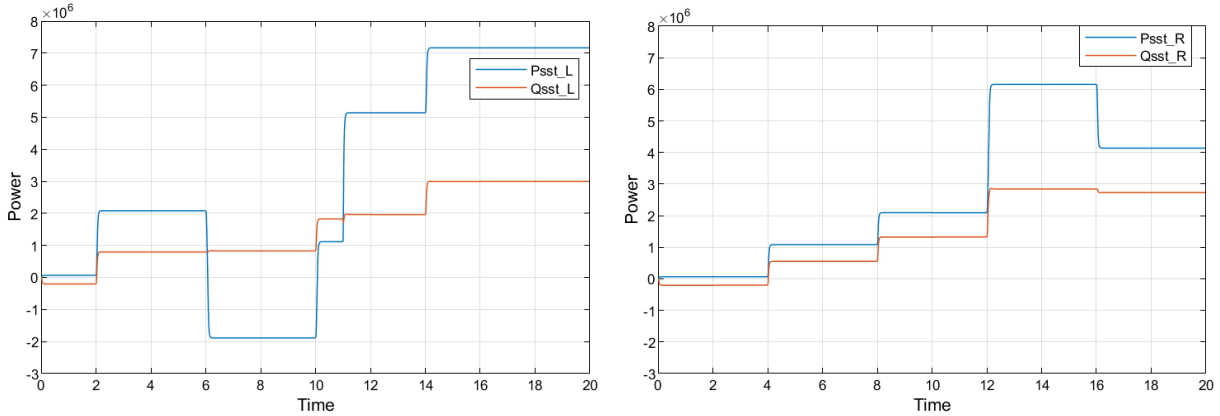


Figure 11. Evolution of the total active and reactive power in the left substation (left) and in the right substation (right).

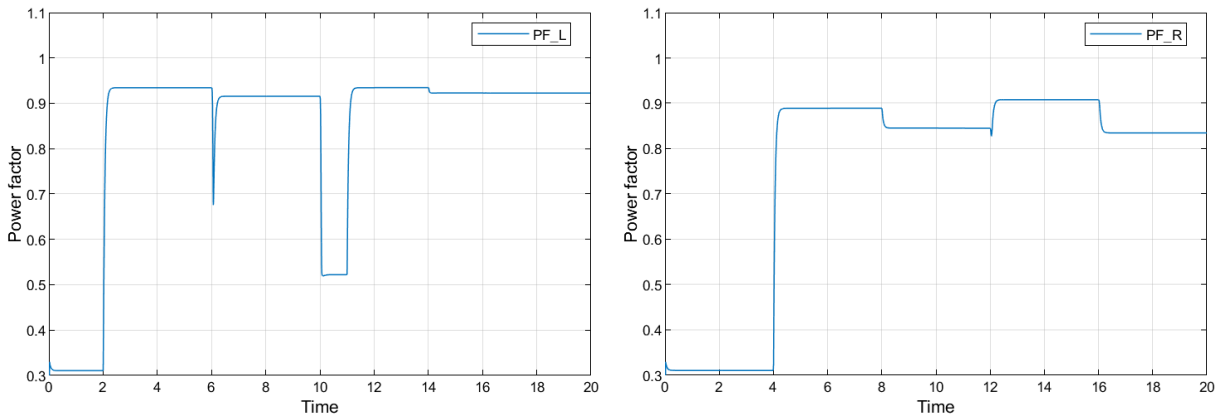


Figure 12. Evolution of the power factor in the left substation (left) and in the right substation (right).

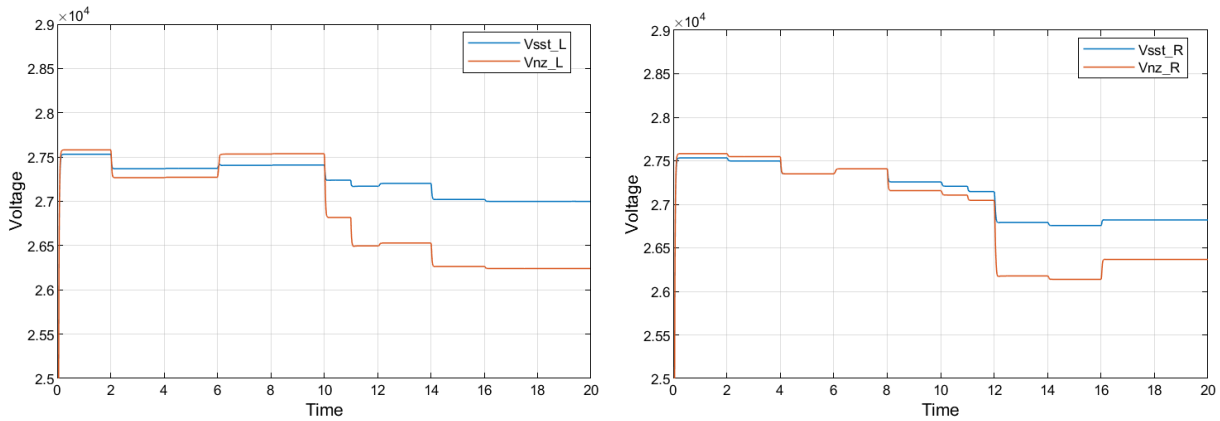


Figure 13. Evolution of left substation voltage and neutral zone voltage (left) and right substation voltage and neutral zone voltage in the right section (right).

The active and reactive power supplied by each substation is approximately the sum of the power demanded by all trains in the line section; the difference is the losses, which are a relevant parameter in electrified railway systems.

Regarding the power factor in the SST, despite the relatively high power factor in all trains, the reactive characteristic of the catenary line imposes a reduction in the SST power factor. Between $t = 10$ s and $t = 11$ s, when a train is in braking mode, the reduction in the total active power demand while maintaining the reactive power causes an important reduction in the substation power factor.

Between $t = 6$ s and $t = 10$ s, we notice an increase in the voltage level in the left neutral zone due to a train in braking mode, but this is the exception. The voltage magnitude at the two points of the neutral zone is reduced according to the load conditions (active and reactive power demand of the trains in their respective sections). The system losses (mainly load-dependent) are also an important parameter for the RIPFC system; they will be shown later in conjunction with the two compensation modes being analysed for comparative purposes.

3.3.2. Power Factor Compensation

One of the RIPFC functionalities demonstrated in this paper is the capability of compensating the reactive power directly in the substation, not only in the neutral zone; this is the main function of a static var compensator. It is used in the same scenario as the one used before: the same number of trains (four) in the left and right sections, the same active and reactive power per train, the same positions on the sections and the same start/stop times (see Figure 10 and Table 3 for details).

In this scenario, the RIPFC does not manage active power; thus, the active power asymmetry between the two sections will be maintained and reflected in the substations. However, the reactive current injected into the PCC (two connections in this case since the compensation is independent on both sides of the neutral zone) for substation compensation will have positive and negative effects. The power factor in the substations will become unitary, and the voltage profile will be more stable. On the contrary, system losses will become higher than in the base scenario.

The following figures show the results for the described scenario: Figure 14 shows the total active and reactive power in both substations.

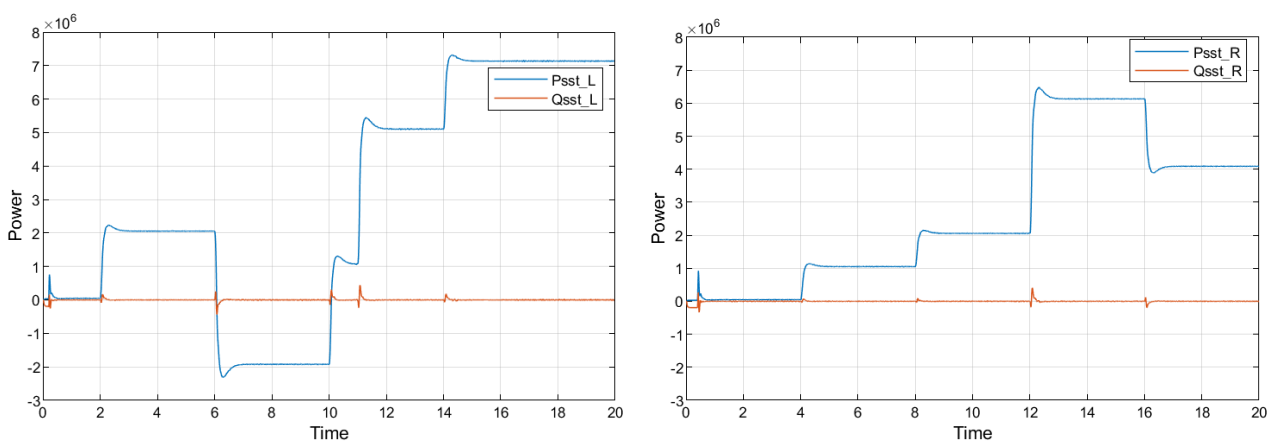


Figure 14. Total active and reactive power in the left substation (**left**) and in the right substation (**right**) with reactive power control in both substations.

Figure 15 shows the voltage profile in each substation and in both sides of the neutral zone.

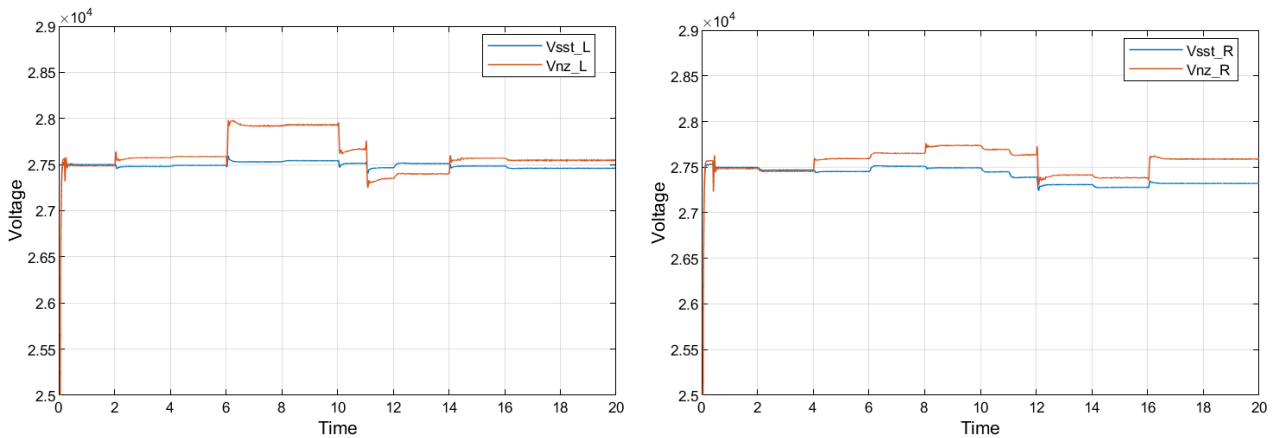


Figure 15. Left substation voltage and neutral zone voltage (**left**) and right substation voltage and neutral zone voltage in the right section (**right**) with reactive power control.

As for the RIPFC system, we show (in Figure 16) the results relative to the active and reactive power (P_c and Q_c) at each connection point.

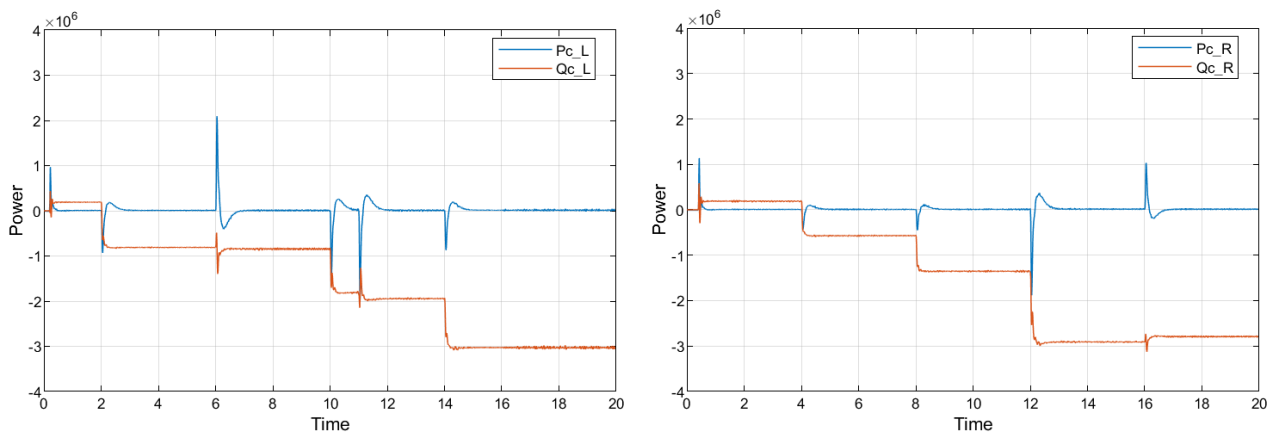


Figure 16. Left converter P_{c_L} and Q_{c_L} (**left**) and right converter P_{c_R} and Q_{c_R} (**right**) requirements with reactive power control.

The compensation for the reactive power in both substations is clear: it becomes zero. Accordingly, the power factor reaches one. Since there is no control of the active power by any means, we have verified that the active power supplied by each substation is nearly the same as in the base case, i.e., with the RIPFC disconnected.

As referred, the other positive effect of compensating the reactive power is the increased voltage stability along the overhead catenary line, which is much more constant if compared with the base case. The RIPFC system is the means to achieve the compensation; it behaves like an SVC at the neutral zone, but its objective is slightly different: it compensates the reactive power at the substation. The reactive power supplied by the RIPFC is also shown, and since the two DC buses are not connected, there is no possibility to manage (redirect) active power; this only occurs in transient conditions.

As referred before, the system losses (in the catenary line, transformers and converters) are an important factor in system operation; the losses for the three analysed scenarios will be compared later in a table.

3.3.3. Active Power Balancing and Double-Side Feeding

Active power balancing is the most important feature of the RIPFC system. It can be used for different purposes, namely transferring active power between two sections of a

line when there is a train in braking mode in one section and regenerative energy is not allowed at the substation. Eventually, there will be trains in traction mode in the other section that can absorb the power coming from the braking train through the RIPFC.

The more general feature of active power redirection is another one: the possibility of operating the two neighbouring substations as if they were in parallel, turning the system into a double-side feeding one. The total active power to be supplied to the trains in the two sections can be divided equally between the two substations. To achieve this, we need measurements of the active power in both substations and a communication link between each substation and the neutral zone where the RIPFC is located. This is an important aspect/requirement to be taken into consideration in the assessment stage of the inclusion of an RIPFC system in a railway system; however, it is out of the scope of this work.

The following results were obtained using the same conditions already used for reactive power compensation only. In this new control mode, the two DC buses are short-circuited and the control algorithm is changed; the common DC bus voltage is controlled by one converter only, and the other converter controls the active power flow in order to satisfy the received command.

Reactive power control in each converter maintains the same objective: that is, imposing a unitary power factor in the substation of the same section. Then, the following figures show the results for the described scenario: total active and reactive power in both substations, voltage profile in each substation and on both sides of the neutral zone, converter active and reactive power (P_c and Q_c) required for the compensation, and estimated power losses in this mode.

Figure 17 shows the total active and reactive power flowing in both substations: Psst_L and Qsst_L for the left substation and Psst_R and Qsst_R for the right substation.

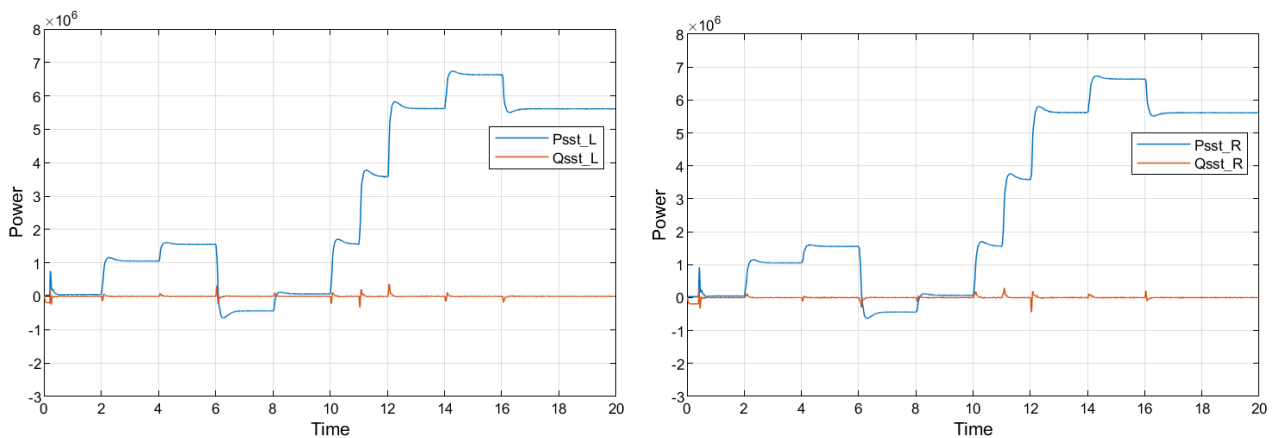


Figure 17. Total active and reactive power in the left substation (left) and in the right substation (right) with active and reactive power control.

Figure 18 shows the voltage profile in each substation and on both sides of the neutral zone when operating in this control mode: Vsst_L and Vnz_L for the left substation and neutral zone, and Vsst_R and Vnz_R for the right substation and neutral zone, respectively.

As for the converters in the RIPFC system, we show (in Figure 19) the results relative to the active and reactive power requirements (P_c and Q_c) at each connection point.

From the above results, it is clear that the compensation of the reactive power in both substations is as before. Accordingly, the power factor reaches one in all conditions.

The other important and different result is that the two substations become balanced in terms of active power. Also, the voltage stability along the overhead line is maintained. As known, the voltage level is more dependent on the reactive power flow than on the active power flow. Thus, the result does not change too much between the two compensation modes. The active and reactive power flow in the RIPFC system is also shown. As expected, the active power flow is in the opposite direction in the two converters.

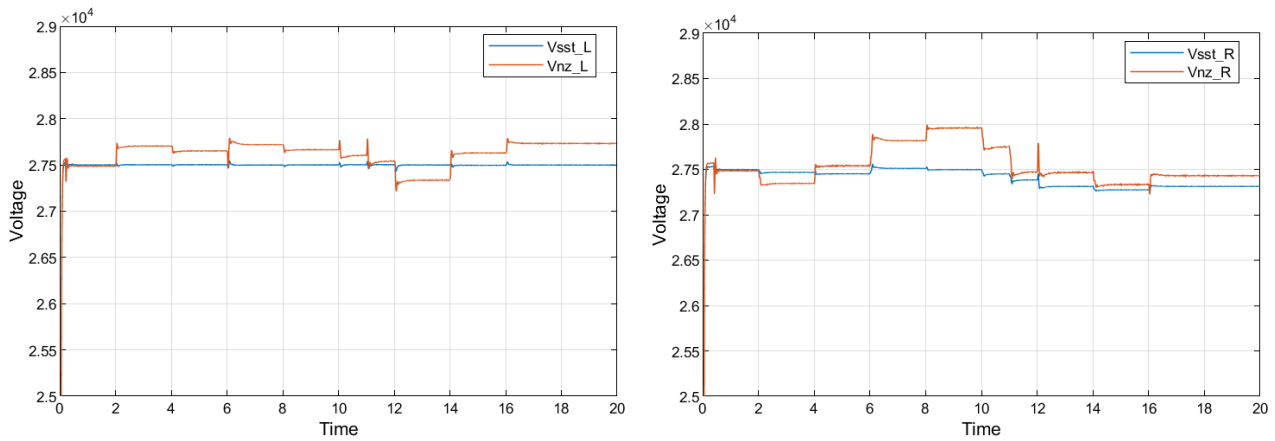


Figure 18. Left substation voltage and neutral zone voltage (**left**) and right substation voltage and neutral zone voltage in the right section (**right**) with active and reactive power control.

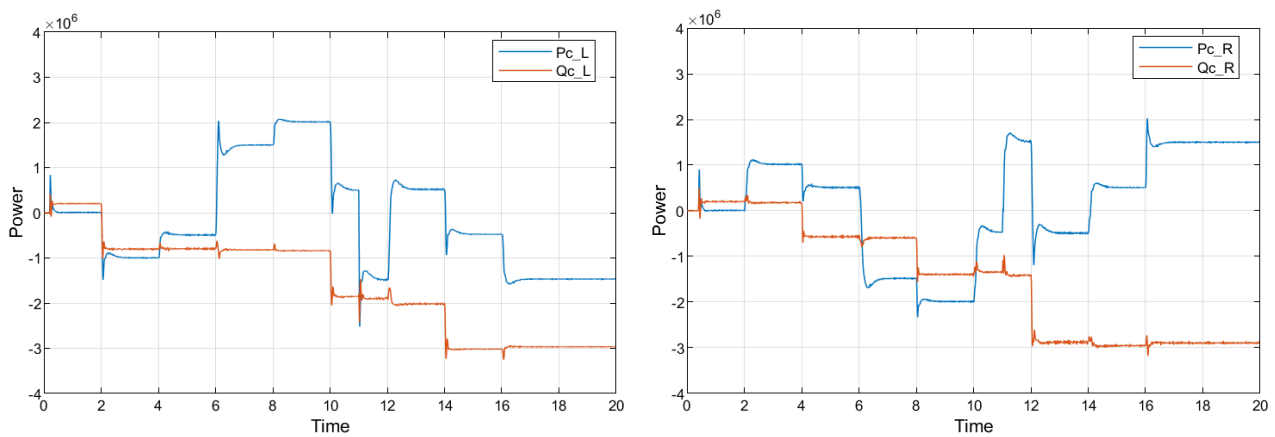


Figure 19. Left converter Pc_L and Qc_L (**left**) and right converter Pc_R and Qc_R (**right**) when compensating the active and reactive power in both substations.

For the three scenarios presented (no compensation, reactive power compensation and full compensation) and for the trains with the powers and positions given earlier in Figure 10 and Table 3, the system losses are given in Table 4.

Table 4. System losses (in kW) in different scenarios: 1—without compensation, 2—power factor compensation, and 3—power factor compensation and active power balancing.

| Scenario | 1-2, (s) | 3-4, (s) | 5-6, (s) | 7-8, (s) | 9-10, (s) | 13-14, (s) | 15-16, (s) | 17-18, (s) |
|----------|----------|----------|----------|----------|-----------|------------|------------|------------|
| 1 | 65 | 66 | 65 | 85 | 87 | 185 | 205 | 165 |
| 2 | 100 | 105 | 105 | 125 | 135 | 240 | 270 | 230 |
| 3 | 100 | 110 | 105 | 125 | 135 | 240 | 270 | 225 |

Comparing the losses in the three scenarios, it can be concluded that in all eight cases, the losses are higher when any type of compensation is made. This should be taken into consideration when assessing the RIPFC in a specific installation and operating condition.

3.3.4. Discussion

The two chosen scenarios demonstrate the RIPFC’s capabilities in terms of reactive power compensation and active power transfer between different sections. The resultant power losses are higher than in the base scenario (no compensation); however, railway operations in real conditions contain a much larger number of scenarios, for which in some

of them, the global losses will become smaller when compensation is made, as shown in [16].

An extensive probabilistic analysis (100,000 cases) was carried out in another research study by the authors of [16], in which the factors considered most-relevant to influencing losses in the system were the type of SST (sparse or dense in terms of the number of trains supplied) and the length of the branch (short or long). The performed analysis used different variables: number of trains in the branch, trains' apparent power and power factor, branch length, and distance to the SST; all the variables were fitted with probability density functions. The system losses included the catenary losses and the RIPFC losses (efficiency level, constant losses and power-dependent losses). The outcomes of the study in [16] in terms of the sparsity/density of the SST type are as follows:

- When both SSTs are sparse, the probability of having a favourable scenario (i.e., lower system losses) is just 0.7% on average;
- If one SST is dense, the probability of a favourable case is 19.3% higher than when both SST are sparse; with both SSTs being of the dense type, the probability of a favourable case is 20.8% higher than with both SSTs being sparse.

The results for favourable scenarios regarding the SST branch lengths, in association with the SST type, are summarized as:

- If both SST branches are short, the probability of a positive case is 12.8%; if both SST branches are long, it is 16.8%;
- If both SSTs are dense and one SST branch is different from the other, the probability of a positive case is 22.7%;
- The highest probabilities occur when one SST is dense and short and the other is sparse and long (17.9%) and when one SST is dense and long and the other is sparse and short (23.4%).

From the above results, we can conclude that system losses could be an important issue when considering the installation of an RIPFC system in a real line. The next subsection provides a systematized reduced scenario for better insight into this issue.

3.4. Reduced Scenario

The presented reduced scenario is intended to better demonstrate cases wherein the system losses become smaller when using the RIPFC system than without it. For this, the selected scenario has four trains (all in the left section) with the same apparent power: $S = 8 \text{ MW} + j2.62 \text{ MVAR}$, which corresponds to a power factor of 0.95i. The four trains are positioned at distances of $D = 5 \text{ km}$, 15 km , 25 km and 35 km , respectively, from the left substation and run for 3 s, in accordance with Figure 20.

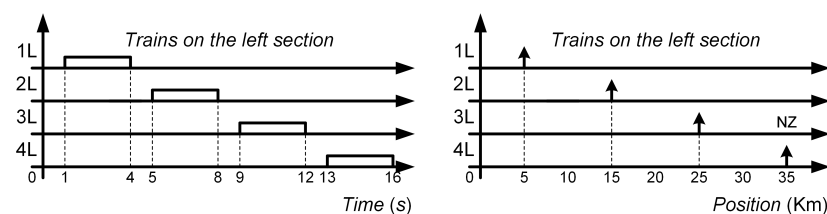


Figure 20. Start/stop times of trains (left) and their positions in the respective sections (right) in a reduced scenario.

3.4.1. Without Compensation

Without compensation, the total active and reactive power of the trains in the two sections is directly observed from the trains' positions and powers: only the left substation supplies power, and it has a power factor very similar to the train's. The voltage profile in each substation and neutral zone is given in Figure 21.

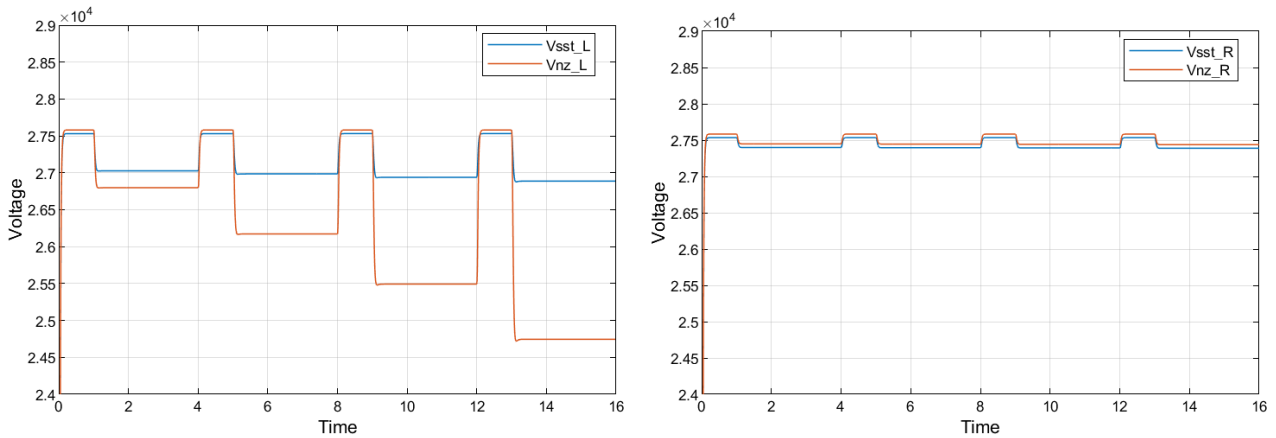


Figure 21. Left substation voltage and neutral zone voltage (**left**) and right substation voltage and neutral zone voltage in the right section (**right**) in a reduced scenario and without compensation.

The losses in this reduced scenario without compensation will be shown in a table in conjunction with the losses when applying full compensation.

Of relevance, it is worth mentioning the small reduction in the left substation power factor according to the train distance to the substation and the relevant reduction in the voltage magnitude at the neutral zone when the train is close to it; both are expected results, as demonstrated before.

3.4.2. With Compensation

When the RIPFC is used for active and reactive power flow control in the substations for this reduced scenario, the main results obtained are shown in the following figures; the same sequence as before is used to show the results. The total active and reactive power in both substations using the RIPFC is given in Figure 22. According to the compensation strategy, the power factor in both substations becomes almost unitary.

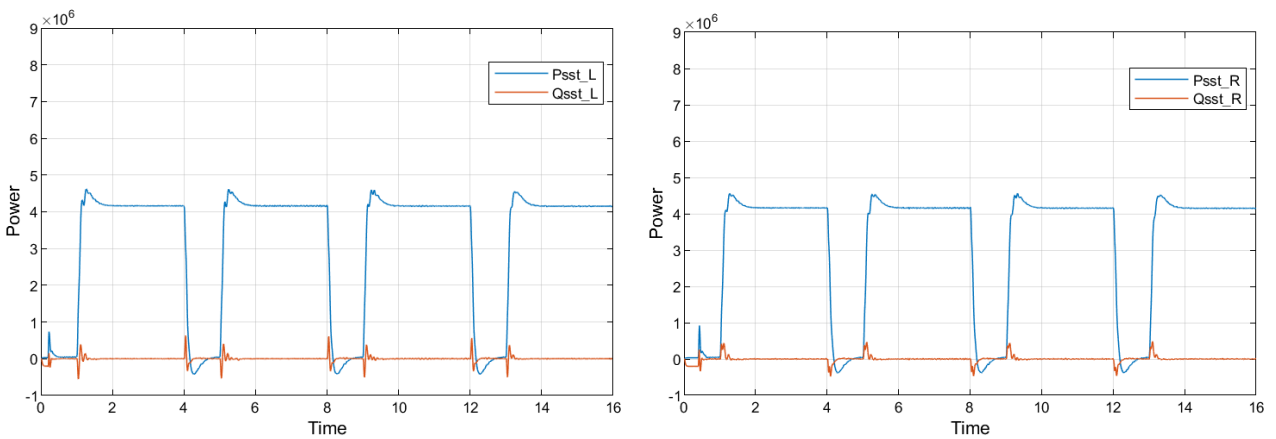


Figure 22. Total active and reactive power in the left substation (**left**) and in the right substation (**right**) with the RIPFC system in full compensation mode (reduced scenario).

The voltage profile in each substation and associated neutral zone is shown in Figure 23; the converter’s active and reactive power requirements (P_c and Q_c) for both sides appears in Figure 24).

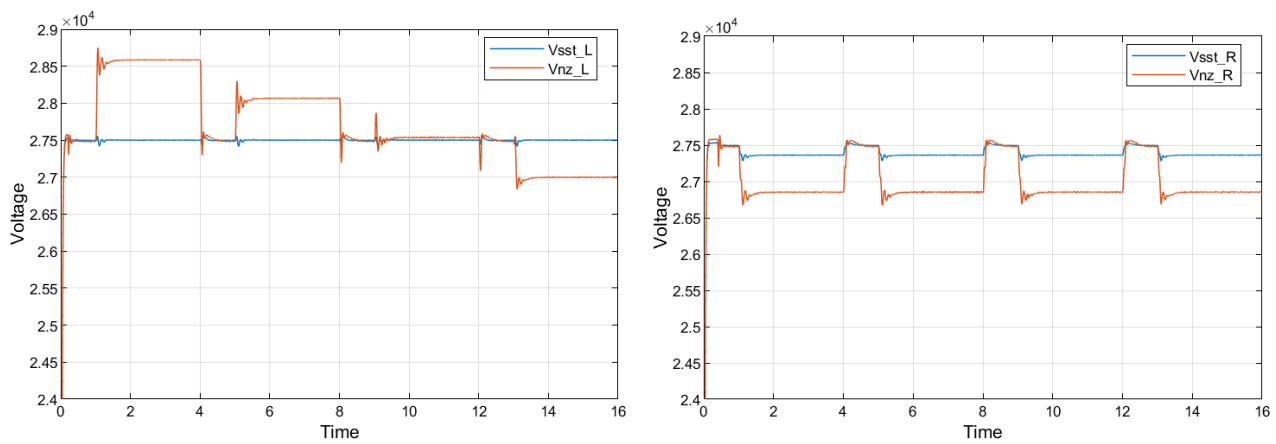


Figure 23. Left substation voltage and neutral zone voltage (**left**) and right substation voltage and neutral zone voltage in the right section (**right**) with the RIPFC in full mode (reduced scenario).

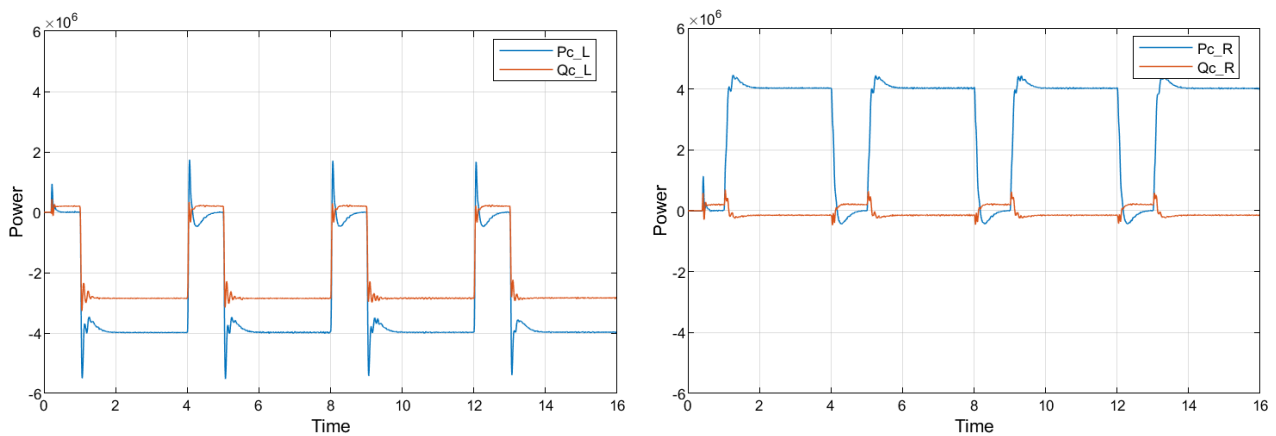


Figure 24. Left converter P_{c_L} and Q_{c_L} (**left**) and right converter P_{c_R} and Q_{c_R} requirements (**right**) when compensating active and reactive power in both substations (reduced scenario).

Finally, the estimated power losses in the reduced scenario and in full compensation mode are shown in Table 5 along with the losses without compensation for comparison.

Table 5. System losses (in kW) in different scenarios: 1—without compensation; 2—full compensation.

| Scenario | 2-4, (s) | 6-8, (s) | 10-12, (s) | 14-16, (s) |
|----------|----------|----------|------------|------------|
| 1 | 100 | 205 | 330 | 460 |
| 2 | 325 | 320 | 310 | 300 |

The conclusions that can be obtained for the presented reduced scenario are as follows: active power balancing is achieved and both substations become evenly loaded: that is, the right substation supplies nearly $P_{SST_L} = 4$ MW to the train in the left section; as before, the power factor at each substation becomes equal to one; much more stable voltage is obtained in the left neutral zone; the left side of the RIPFC must manage active power (it receives power from the DC bus side and supplies it to the AC side) and supply reactive power to compensate the substation power factor.

In terms of power losses, it can be observed that they are almost constant, independent of the trains' positions. In the first two positions (closer to the left substation), the estimated losses are higher than the ones in the scenario without the RIPFC, and the losses are slightly smaller in the third position. However, the losses are smaller in the last condition, where the train is closer to the neutral zone. This is a general result; the introduction of the

RIPFC system adds constant losses to the system (mainly associated with the transformers' magnetization losses) and current/power-dependent losses (transformers, converters and catenary). The current associated with the transferred power increases the losses in one section and reduces them in the other section; thus, there are conditions for which the total losses can be smaller with the RIPFC than without it. It should be mentioned that additional work related to the sp-RPC/PTD/RIPFC system has been performed using statistical models and probability distributions, with the general conclusions being very similar to the ones discussed here [16].

4. Discussion

Regarding reactive power compensation, we proposed to compensate the power factor at the substation instead of the voltage magnitude at the neutral zone, and this is the main contribution of this paper. The opposite could be selected: nearly constant voltage at the weakest connecting point (the neutral zone) would be achieved but with the negative impact of a lower power factor at the substation level. This is the same feature of an SVC connected to the neutral zone; the presented approach adds flexibility to the system: giving the infrastructure manager a degree of freedom.

When redirecting active power between the two sections while maintaining the compensation of reactive power in the substation, a double-side feeding condition is achieved, i.e., both neighbouring substations supply the same active power but, as pointed out before, a different sharing factor is possible if a specific requirement is received from a supervisory layer.

There are two topics not addressed in this work that should be considered for further analysis: (i) the need for substation measurements and communication links between the substation SCADA system and the RIPFC control system and (ii) the trade-off between system power losses (in the catenary, transformer and converter) and double-side feeding; in some cases, the system losses become higher with the RIPFC system.

The final assessment of the use of the RIPFC system must be made by considering its important advantages for the electric traction system (unitary power factor at the substation or voltage stabilization at the neutral zone, and double-side feeding effect) and possible weaknesses (communication link and system losses).

5. Conclusions

This paper proposes a new control strategy applied to the railway interline power flow controller: reactive power compensation at the substation level instead of the usual approach of voltage stabilization at the neutral zone. Simultaneously, the other capability of the RIPFC to transfer active power between two sections of a railway line separated by a neutral zone is maintained. In all analysed cases (pseudo-random and reduced scenarios), independently of the number of trains in each section and their traction/braking conditions, the RIPFC achieves unitary power factor at the substation and stabilizes the catenary voltage in the whole section within a very small range.

Analysis of the total losses in the system shows that in most cases, the inclusion of the RIPFC increases the losses; therefore, a trade-off assessment must be performed when considering the adoption of such a system in a real application.

Author Contributions: Conceptualization, A.P.M. and V.A.M.; methodology, A.P.M. and V.A.M.; software, A.P.M.; validation, A.P.M. and V.A.M.; formal analysis, A.P.M.; investigation, A.P.M.; resources, A.P.M.; data curation, A.P.M.; writing—original draft preparation, A.P.M.; writing—review and editing, A.P.M. and V.A.M.; visualization, V.A.M.; supervision, A.P.M.; project administration, A.P.M.; funding acquisition, A.P.M. All authors have read and agreed to the published version of the manuscript.

Funding: This project received funding from the European Union's Horizon 2020 research and innovation programme under grant agreement No 777515 (project In2Stempo).

Institutional Review Board Statement: Not applicable.

Informed Consent Statement: Not applicable.

Data Availability Statement: The data are contained within the article.

Conflicts of Interest: The authors declare no conflicts of interest.

Abbreviations

The following abbreviations are used in this manuscript:

| | |
|---------|---|
| AC | Alternating Current |
| DC | Direct Current |
| EHV | Extra-High Voltage |
| HV | High Voltage |
| NZ | Neutral Zone |
| PCC | Point of Common Coupling |
| PI | Proportional Integral |
| PF | Power Factor |
| PTD | Power Transfer Device |
| PWM | Pulse Width Modulation |
| RIPFC | Railway Interline Power Flow Controller |
| RPC | Rail Power Conditioner |
| SCADA | Supervisory Control And Data Acquisition |
| SST | Substation |
| SVC | Static Var Compensator |
| TSO/DSO | Transmission System Operator/Distribution System Operator |

References

- Liao, J.; Mastoi, M.S.; Wang, D.; Sheng, S.; Zhou, X.; Haris, M. Research on integrated control strategy of doubly-fed induction generator-based wind farms on traction power supply system. *IET Power Electron.* **2022**, *15*, 1340–1349. [[CrossRef](#)]
- Li, Z.; Li, X.; Lin, Y.; Wei, Y.; Li, Z.; Li, Z.; Lu, C. Active disturbance rejection control for static power converters in flexible AC traction power supply systems. *IEEE Trans. Energy Convers.* **2022**, *37*, 2851–2862. [[CrossRef](#)]
- Song, Y.; Ronnquist, A.; Jiang, T.; Navik, P. Railway pantograph-catenary interaction performance in an overlap section: Modeling, validation, and analysis. *J. Sound Vib.* **2023**, *548*, 117506. [[CrossRef](#)]
- Shimada, M.; Oishi, R.; Araki, D.; Nakamura, Y. Energy storage system for effective use of regenerative energy in electrified railways. *Hitachi Rev.* **2010**, *59*, 33–38.
- González-Gil, A.; Palacin, R.; Batty, P. Sustainable urban rail systems: Strategies and technologies for optimal management of regenerative braking energy. *Energy Convers. Manag.* **2013**, *75*, 374–388. [[CrossRef](#)]
- Khodaparastan, M.; Mohamed, A.; Brandauer, W. Recuperation of regenerative braking energy in electric rail transit systems. *IEEE Trans. Intell. Transp. Syst.* **2019**, *20*, 2831–2845. [[CrossRef](#)]
- Lu, Q.; Gao, Z.; He, B.; Che, C.; Wang, C. Centralized-decentralized control for regenerative braking energy utilization and power quality improvement in modified AC-fed railways. *Energies* **2020**, *13*, 2582. [[CrossRef](#)]
- Sutherland, P.; Waclawiak, M.; McGranaghan, M. System impacts evaluation of a single-phase traction load on a 115-kV transmission system. *IEEE Trans. Power Deliv.* **2006**, *21*, 837–844. [[CrossRef](#)]
- IEC. IEC 61000-3-7, *Electromagnetic Compatibility (EMC)—Part 3-7: Limits-Assessment of Emission Limits for the Connection of Fluctuating Installations to MV, HV and EHV Power Systems*; IEC: Geneva, Switzerland, 2008.
- Hayashiya, H. Recent trend of regenerative energy utilization in traction power supply system in Japan. *Urban Rail Transit* **2017**, *3*, 183–191. [[CrossRef](#)]
- Aoki, K.; Kikuchi, K.; Seya, M.; Kato, T. Power interchange system for reuse of regenerative electric power. *Hitachi Rev.* **2018**, *67*, 71–75.
- Gao, Z.; Lu, Q.; Wang, C.; Fu, J.; He, B. Energy-storage-based smart electrical infrastructure and regenerative braking energy management in AC-fed railways with neutral zones. *Energies* **2019**, *12*, 4053. [[CrossRef](#)]
- Perin, I.; Walker, G.; Ledwich, G. Load sharing and wayside battery storage for improving AC railway network performance, with generic model for capacity estimation, Part 1. *IEEE Trans. Ind. Electron.* **2019**, *66*, 1791–1798. [[CrossRef](#)]
- Hayashiya, H.; Kondo, K. Recent trends in power electronics applications as solutions in electric railways. *IEEE Trans. Electr. Electron. Eng.* **2020**, *15*, 632–645. [[CrossRef](#)]
- Pilo, E.; Mazumder, S.; González-Franco, I. Smart electrical infrastructure for AC-fed railways with neutral zones. *IEEE Trans. Intell. Transp. Syst.* **2015**, *16*, 642–652. [[CrossRef](#)]
- Morais, V.; Martins, A. Traction power substation balance and losses estimation in AC railways using a power transfer device through Monte Carlo analysis. *Railw. Eng. Sci.* **2022**, *30*, 71–95. [[CrossRef](#)]

17. Hassan, M.; Hinze, C. FACTS as basis of smart traction power supply systems with 50 Hz nominal frequency. *Eng. Rail Power Supply* **2021**, *119*, 202–209.
18. Hitachi, Ltd. Control Device for Railway Power Conditioner and Control System for Railway Power Conditioner. U.S. Patent 9 573 489 B2, 21 February 2017.
19. Mochinaga, Y.; Takeda, M.; Hasuike, K. Static power conditioner using GTO converters for AC electric railway. In Proceedings of the Conference Record of the Power Conversion Conference, Yokohama, Japan, 19–21 April 1993; pp. 641–646.
20. He, Z.; Zheng, Z.; Hu, H. Power quality in high-speed railway systems. *Int. J. Rail Transp.* **2016**, *4*, 71–97. [[CrossRef](#)]
21. Kaleybar, H.; Brenna, M.; Foadelli, F.; Fazel, S.; Zaninelli, D. Power quality phenomena in electric railway power supply systems: An exhaustive framework and classification. *Energies* **2020**, *13*, 6662. [[CrossRef](#)]
22. Banerjee, S.; Hempel, M.; Sharif, H. A survey of wireless communication technologies and their performance for high speed railways. *J. Transp. Technol.* **2016**, *6*, 15–29. [[CrossRef](#)]
23. Kawahara, K.; Hisamizu, Y.; Hase, S.; Mochinaga, Y. Development of a static Var compensator for San-yo Shinkansen. *Q. Rep. Railw. Tech. Res. Inst.* **2000**, *41*, 148–153. [[CrossRef](#)]
24. Uzuka, T.; Ikedo, S.; Ueda, K. A static voltage fluctuation compensator for AC electric railway. In Proceedings of the IEEE 35th Annual Power Electronics Specialists Conference, Aachen, Germany, 20–25 June 2004; Volume 3, pp. 1869–1873.
25. CENELEC, EN50388-1; Railway Applications—Power Supply and Rolling Stock—Technical Criteria for the Coordination between Power Supply (Substation) and Rolling Stock to Achieve Interoperability. CENELEC: Brussels, Belgium, 2017.
26. Bahrani, B.; Rufer, A.; Kenzelmann, S.; Lopes, L. Vector control of single-phase voltage-source converters based on fictive-axis emulation. *IEEE Trans. Ind. Appl.* **2011**, *47*, 831–840. [[CrossRef](#)]

Disclaimer/Publisher’s Note: The statements, opinions and data contained in all publications are solely those of the individual author(s) and contributor(s) and not of MDPI and/or the editor(s). MDPI and/or the editor(s) disclaim responsibility for any injury to people or property resulting from any ideas, methods, instructions or products referred to in the content.